Journal of Solid State Chemistry 182 (2009) 3162–3170

Contents lists available at ScienceDirect

Journal of Solid State Chemistry

journal homepage: www.elsevier.com/locate/jssc

The d^{10} metal-sulfosalicylate complexes: Herring-bone, ladder and double-stranded chain frameworks with green luminescences

Chun-Feng Yan [a,b], Fei-Long Jiang [a], Lian Chen [a], Rui Feng [a,b], Ming Yang [a,b], Mao-Chun Hong [a,*]

[a] Key Laboratory of Optoelectronic Materials Chemistry and Physics, Fujian Institute of Research on the Structure of Matter, Chinese Academy of Sciences, Fuzhou 350002, China
[b] Graduate School of Chinese Academy of Science, Beijing, China

ARTICLE INFO

Article history:
Received 9 June 2009
Received in revised form
25 August 2009
Accepted 26 August 2009
Available online 31 August 2009

Keywords:
d^{10} Coordination polymer
5-Sulfo-salicylic acid
Crystal structure
Fluorescent properties

ABSTRACT

Assembly of 5-sulfosalicylic acid (H_3L) and d^{10} transition metal ions (Cd^{II}, Ag^{I}) with the neutral N-donor ligands produces five new complexes: $[Cd_2(HL)_2(4,4'\text{-bipy})_3]_n \cdot 2nH_2O$ (**1**), $\{[Cd_2(\mu_2\text{-}HCO_2)_2(4,4'\text{-bipy})_2(H_2O)_4][Cd(HL)_2(4,4'\text{-bipy})(H_2O)_2]\}_n$ (**2**), $\{[Cd(4,4'\text{-bipy})(H_2O)_4][HL]\cdot H_2O\}_n$ (**3**), $[Cd(HL)(dpp)_2(H_2O)]_n \cdot 4nH_2O$ (**4**), $\{[Ag(4,4'\text{-bipy})][Hhbs]\}_n$ (**5**) (4,4′-bipy=4,4′-bipyridine, dpp=1,3-di(pyridin-4-yl)propane, H_2hbs=4-hydroxybenzenesulfonic acid, the decarboxylation product of H_3L). Complex **1** adopts a 5-connected 3D bilayer topology. Complex **2** has the herring-bone and ladder chain, which are extended to a 3D network via hydrogen bonding. In **3–4** complexes, **3** is a 3D supermolecular structure formed by polymeric chains and 2D network of HL^{2-}, while **4** gives the double-stranded chains. In **5**, ladder arrays are stacked with the 2D networks of $Hhbs^-$ anions in an –ABAB– sequence. Complexes **1–4** display green luminescences in solid state at room temperature, while emission spectra of **3** and **4** show obvious blue-shifts at low temperature.

1. Introduction

In recent years, to design and synthesize metal-organic frameworks (MOFs) is one of the most active areas of materials research. The great interest in these materials rests with their fascinating structural diversities [1] and their potential applications as functional materials (photoactive materials [2–9], fluorescent sensor [10], biochemistry [11–14], macromolecular chemistry [15–18], electrical conductivity [19], and so on). Some non-covalent interactions such as π–π stacking [20–22] and hydrogen bonding [23–28], also greatly affect the structures and properties of coordination complexes. In constructing coordination polymers, 5-sulfosalicylic acid (H_3L, Scheme 1) can be recognized as a useful starting material, since H_3L is a polydentate ligand and has three potential coordinating groups ($-CO_2H$, $-SO_3H$ and –OH), which can give mono-, di- and tri-anionic ligand species (H_2L^-, HL^{2-}, L^{3-}) with controlled deprotonation through changes of reaction condition. Therefore, it can coordinate to metal ions with different modes to meet a considerable requirement for the construction [29–34]. And H_3L also tends to provide abundant hydrogen bonding, favoring the formation of the versatile metal-organic frameworks, and linking low-dimensional structures into high-dimensional supramolecular networks. In addition, H_3L has been found to have excellent fluorescence potency [23–27,35]. Some literatures have reported the functional complexes in this aspect, however, the fluorescent studies of the ligand H_3L with d^{10} metal ions, such as cadmium(II) and silver(I), are still relatively rare [29,34].

With the aim of preparing new materials with beautiful architecture and great fluorescence properties, we tend to synthesize a series of d^{10} metal coordination complexes constructed from the primary ligands, H_3L and its decarboxylation product, 4-hydroxybenzenesulfonic acid (H_2hbs). In this article, 4,4′-bipyridine (4,4′-bipy) and 1,3-di(pyridin-4-yl)propane (dpp) have been employed as the ancillary ligands to synthesize five Cd(II) or Ag(I) complexes: $[Cd_2(HL)_2(4,4'\text{-bipy})_3]_n \cdot 2nH_2O$ (**1**), $\{[Cd_2(\mu_2\text{-}HCO_2)_2(4,4'\text{-bipy})_2(H_2O)_4][Cd(HL)_2(4,4'\text{-bipy})(H_2O)_2]\}_n$ (**2**), $\{[Cd(4,4'\text{-bipy})(H_2O)_4][HL]\cdot H_2O\}_n$ (**3**), $[Cd(HL)(dpp)_2(H_2O)]_n \cdot 4nH_2O$ (**4**), $\{[Ag(4,4'\text{-bipy})][Hhbs]\}_n$ (**5**). The H_3L ligand shows three different coordination modes I, II, and III (Scheme 2) in above complexes. These luminescent d^{10} metal-sulfosalicylate complexes show the interesting structures, such as herring-bone, ladder and double-stranded chain frameworks. Here we wish to report their syntheses, structures and luminescent properties.

2. Experimental section

2.1. Materials and physical measurements

Chemicals were commercially purchased and used as received. Hydrothermal syntheses were carried out in Teflon-lined

* Corresponding author. Fax: +86 591 83794946.
E-mail address: hmc@fjirsm.ac.cn (M.-C. Hong).

0022-4596/$ - see front matter © 2009 Elsevier Inc. All rights reserved.
doi:10.1016/j.jssc.2009.08.025

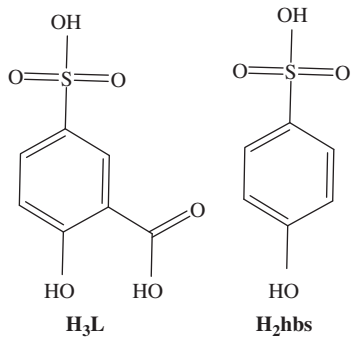

H_3L H_2hbs

Scheme 1. Schematic representation of primary and ancillary ligands.

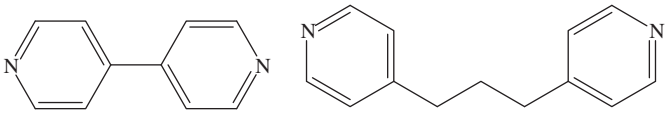

4,4'-bipy dpp

Scheme 2. Different coordination modes of 5-sulfosalicylate in complexes **1–4**.

stainless-steel autoclaves under autogenous pressure. Fluorescent spectra were measured on an Edinburgh Instruments analyzer model FLS920 with 450 W xenon light. IR spectra were recorded with KBr disks in range 4000–400 cm^{-1} on a Perkin-Elmer Spectrum One FT-IR Spectrometer. Thermal gravimetric analyses (TGA) were performed with a heating rate of 10 °C min^{-1} using a NETZSCH STA 449C simultaneous TG-DSC instrument. Elemental analyses were carried out on an Elementar Vario EL III micro-analyzer. Powder X-ray diffraction (PXRD) data were collected on a Rigaku DMAX2500 diffractometer.

2.2. Preparation of $[Cd_2(HL)_2(4,4'\text{-bipy})_3]_n \cdot 2nH_2O$ (**1**)

$CdCO_3$ (0.110 g, 0.5 mmol) was added to 10 mL aqueous solution of H_3L (0.109 g, 0.5 mmol) and heated at 100 °C under stirring until $CdCO_3$ power dissolved completely. 4,4′-bipy (0.195 g, 1.25 mmol) was added, and the mixture was sealed into a bomb equipped with a Teflon liner and then was heated at 150 °C for 72 h. Colorless brick-shaped crystals of complex **1** suitable for single crystal X-ray analysis were obtained. Yield: 84.8% (0.123 g) based on Cd. Anal. for $C_{44}H_{32}N_6O_{14}S_2Cd_2$ (%). Found for complex **1**: C, 45.38; H, 3.11; N, 7.25. Calcd: C, 45.36; H, 3.12; N, 7.22. IR data (KBr, cm^{-1}): 3396s, 3050w, 1599vs, 1575m, 1536m, 1486s, 1447s, 1412s, 1385w, 1287w, 1221s, 898m, 801s, 726m, 672s.

2.3. Preparation of $\{[Cd_2(\mu_2\text{-}HCO_2)_2(4,4'bipy)_2(H_2O)_4][Cd(HL)_2(4,4'\text{-}bipy)(H_2O)_2]\}_n$ (**2**)

To the colorless solution of H_3L (0.218 g, 1 mmol) in 30 mL MeCN, sodium methoxide (NaOMe, 0.162 g, 3 mmol) was added, and the mixture turned into white suspension. Subsequently, $Cd(NO_3)_2 \cdot 4H_2O$ (0.024 g, 1 mmol) was added into the above mixture. After about half an hour, 4,4′-bipy (0.156 g, 1 mmol) was added. The reaction mixture was kept stirring for 6 h and filtered out. The filter residue was then resolved in DMF. After two months evaporation, yellow block crystals of complex **2** suitable for single crystal X-ray analysis were isolated and air-dried. Yield: 37.5% (0.180 g) based on Cd. Found for complex **2**: C, 38.44; H, 3.21; N, 5.87. Calcd: C, 38.47; H, 3.23; N, 5.85. IR data (KBr, cm^{-1}): 3416s, 3050w, 1603vs, 1633w, 1583m, 1490m, 1447m, 1416m, 1385w, 1276w, 1221s, 894w, 805s.

2.4. Preparation of $\{[Cd(4,4'\text{-bipy})(H_2O)_4][HL] \cdot H_2O\}_n$ (**3**)

The reaction procedure was the same as that of complex **1** except that 120 °C/6 days was used instead of 150 °C/72 h. Colorless brick-shaped crystals of complex **3** suitable for single crystal X-ray analysis were obtained. Yield: 68.6% (0.197 g) based on Cd. Anal. for $C_{17}H_{22}N_2O_{11}SCd$ (%). Found for complex **3**: C, 36.05; H, 3.73; N, 4.86. Calcd: C, 35.52; H, 3.86; N, 4.87. IR data (KBr, cm^{-1}): 3443vs, 3056m, 2921m, 2848m, 1602vs, 1574s, 1488m, 1446m, 1415m, 1384m, 1256w, 1219vs, 1178vs, 1126m, 1075m, 1034s, 1003m, 890w, 820w, 806s, 723w.

2.5. Preparation of $[Cd(HL)(dpp)_2(H_2O)]_n \cdot 4nH_2O$ (**4**)

$CdCO_3$ (0.110 g, 0.5 mmol) was added to 10 mL aqueous solution of H_3L (0.109 g, 0.5 mmol) and heated at 100 °C under stirring until $CdCO_3$ power dissolved completely. The dpp (0.099 g, 0.5 mmol) was added, and the resultant mixture was sealed into a bomb equipped with a Teflon liner and then was heated at 120 °C for 6 days. Colorless brick-shaped crystals of complex **4** suitable for single crystal X-ray analysis were obtained. Yield: 40.1% (0.150 g) based on Cd. Anal. for $C_{33}H_{41}N_4O_{11}SCd$ (%). Found for complex **4**: C, 48.65; H, 5.11; N, 6.65. Calcd: C, 48.68; H, 5.08; N, 6.88. IR data (KBr, cm^{-1}): 3451vs, 3054m, 2925m, 2852m, 1613s, 1579m, 1501w, 1447m, 1260w, 1209s, 1176s, 1034s, 1011w, 890w, 809m, 789w, 746w.

2.6. Preparation of $\{[Ag(4,4'\text{-bipy})][Hhbs]\}_n$ (**5**)

A mixture of H_3L (0.109 g, 0.5 mmol), $AgBF_4$ (0.097 g, 0.5 mmol) and 4,4′-bipy (0.078 g, 0.5 mmol) in 42-mL Teflon-lined stainless-steel vessel was heated at 150 °C for 5 days, giving colorless prismatic crystals of **5**. Yield: 61.8 % (0.135 g) based on Ag. Anal. for $C_{16}H_{13}N_2O_4SAg$ (%). Found for complex **5**: C, 43.80; H, 3.26; N, 6.58. Calcd: C, 43.95; H, 3.00; N, 6.41. IR data (KBr, cm^{-1}): 3566m, 3046m, 1956w, 1599s, 1532m, 1505m, 1432m, 1410s, 1209vs, 1178vs, 743m, 806vs.

3. X-ray crystallography

Intensity data were collected on a Rigaku mercury CCD diffractometer with graphite-monochromated Mo *Ka* (λ=0.71073 Å) radiation by using ω-2θ scan method at room temperature. The structures were solved by direct methods using SHELXS-97 and were refined on F^2 by full-matrix least-squares methods using SHELXL-97 [36,37]. All non-hydrogen atoms were refined anisotropically and the hydrogen atoms were treated as idealized contributions except those on water molecules and the shared ones. A summary of the crystallographic data of complexes **1–5** are listed in Table 1, and their selected bond lengths and angles are tabulated in Table 2, respectively.

4. Results and discussion

4.1. Syntheses

H_3L molecule has desirable stereochemical features with its three potential coordinating groups and gives multidentate coordination through controlling of reaction temperature, reactant stoichiometry and ancillary ligands. Complexes **1**, **3–5** were

Table 1
Crystallographic data for complexes **1**–**5**.

Complex	**1**	**2**	**3**	**4**	**5**
Empirical formula	$C_{22}H_{16}N_3O_7SCd$	$C_{46}H_{46}N_6O_{22}S_2Cd_3$	$C_{17}H_{22}N_2O_{11}SCd$	$C_{33}H_{41}N_4O_{11}SCd$	$C_{16}H_{13}N_2O_4SAg$
Formula weight	580.88	1436.26	574.83	814.16	437.21
Crystal size (mm)	0.30 × 0.12 × 0.09	0.10 × 0.10 × 0.05	0.20 × 0.15 × 0.10	0.10 × × 0.06 × 0.04	0.40 × 0.20 × 0.10
Crystal system	Monoclinic	Monoclinic	Monoclinic	Triclinic	Triclinic
Space group	*C*2/*c*	*C*2/*c*	*P*2$_1$/*c*	*P*-1	*P*-1
Unit cell parameters	*a*=22.988(8) Å	*a*=20.329(1) Å	*a*=6.921(3) Å	*a*=9.314(3) Å	*a*=8.017 Å
	b=10.986(4) Å	*b*=11.645(7) Å	*b*=26.786(10) Å	*b*=12.252(4) Å	*b*=10.410 Å
	c=18.298(7) Å	*c*=21.606(12) Å	*c*=11.644(4) Å	*c*=17.834(6) Å	*c*=11.007 Å
	α=90°	*α*=90°	*α*=90°	*α*=104.811(4)°	*α*=117.91°
	β=111.342(6)°	*β*=91.508(11)°	*β*=91.407(5)°	*β*=92.165(10)°	*β*=94.55°
	γ=90°	*γ*=90°	*γ*=90°	*γ*=109.648(4)°	*γ*=104.81°
Volume (Å^3)	4304 (3)	5113 (5)	2158.0 (14)	1835.8 (10)	763.2
Z	8	4	4	2	2
D_{calcd} (g/cm^3)	1.787	1.866	1.769	1.473	1.902
μ (mm^{-1})	1.164	1.408	1.171	0.714	1.481
F(000)	2288	2864	1160	838	436
Reflns. collected	16205	19252	15814	10335	5866
Reflns. unique	4909	5842	4816	5105	3437
Final *R*, *wR* indices ($I > 2\sigma(I)$)	0.0497	0.0462	0.0438	0.0551	0.0287
	0.1338	0.1179	0.1029	0.1598	0.0692
Max, min$\Delta\rho$ (eÅ^{-3})	0.927, −1.374	0.864, −0.944	0.910, −0.306	1.016, −1.057	0.691, −0.506

prepared under hydrothermal conditions (150–100 °C), while complex **2** was prepared under aquicultural condition at room temperature. Among them, complexes **3–4** with different structural features were obtained using different ancillary ligands (4,4′-bipy or dpp) at the same reaction temperatures. And complexes **1** and **3** were synthesized with similar reaction procedures but at different reaction temperatures and time. Obviously, the ancillary ligands, reaction temperature and time all play important roles in resulting products for this system. HL^{2-} ligands and ancillary ligands in **1–2**, **4** complexes all coordinate to central metal ions, and HL^{2-} ligands here appear three kinds of coordination modes (Scheme 2). For complexes **3** and **5**, ligands of HL^{2-} and $Hhbs^-$ only act as counter anions for charge balance, while 4,4′-bipy ligands participate in coordinating to metal centers. The above-mentioned complexes all give single-phase blocks. Phase purity was judged by elemental analysis and PXRD via comparison with spectra predicted from single-crystal structural determinations.

4.2. Crystal structures

4.2.1. $[Cd_2(HL)_2(4,4'\text{-bipy})_3]_n \cdot 2nH_2O$ (**1**)

As revealed by single-crystal X-ray diffraction, in the asymmetric unit of **1**, each of Cd(II) center adopts a distorted octahedral geometry and is six-coordinated by one sulfonate oxygen atom, two carboxylate oxygen atoms from two different HL^{2-} ligands, and three nitrogen atoms from three 4,4′-bipy ligands (Fig. 1). The Cd1–O1, Cd1–O2 and Cd1–O4 bonds are 2.419 (3), 2.344 (3) and 2.292 (3) Å, respectively, and Cd1–N bonds exit in the range of 2.311 (4) and 2.365 (3) Å. With coordination mode I for HL^{2-} ligands as the bridges in **1**, both $-SO_3H$ and $-CO_2H$ groups of HL^{2-} ligand are deprotonated and coordinate to metal centers, while –OH group of HL^{2-} keeps neutral. Cd(II) centers are connected by HL^{2-} and 4,4′-bipy ligands to form a two-dimensional network, as shown in Fig. 2a, which is further linked to form a three-dimensional supermolecular structure through 2-fold interpenetration (Fig. 2b). The resulting array is a 5-connected network, and two parallel 4^4 nets are linked through the single bridging 4,4′-bipy molecules for the two-dimensional bilayers structure (Fig. 3a). And these two-dimensional bilayer structures further form a three-dimensional network through 2-fold interpenetration (Fig. 3b). The coordination modes of HL in **1** are different from the reported coordination complexes with 2,2′-bipy or (1,4-bis(imidazol-1-ylmethyl)-benzene) as ancillary ligands, $[Cd_3(1,4\text{-bis(imidazol-1-ylmethyl)-benzene})_3(L)_2(H_2O)_4]_n$ [29] and $[Cd(HL)(2,2'\text{-bipy})]_n$ [38].

4.2.2. $\{[Cd_2(\mu_2\text{-}HCO_2)_2(4,4'\text{-bipy})_2(H_2O)_4][Cd(HL)_2(4,4'\text{-bipy})(H_2O)_2]\}_n$ (**2**)

The structure of complex **2** is much different from complex **1**, and is a one-dimensional supermolecular structure formed with two different and unattached infinite chains. There are two crystallographically unique Cd(II) centers in **2**, and both of them take six-coordinated environments. In Cd1 center, Cd1 exhibits a distorted octahedral coordinated by two oxygen atoms (Cd1–O6 2.320 (3) Å, Cd1–O6A 2.320 (3) Å) of carboxyl groups from two different HL^{2-} ligands, two nitrogen atoms (Cd1–N1 2.261 (4)Å, Cd1–N2 2.289 (5) Å) from two different 4,4′-bipy ligands, and two other oxygen atoms (Cd1–O7 2.326(4)Å, Cd1–O7A 2.326 (4) Å) from water molecules. These Cd1 centers are bridged by 4,4′-bipy ligands to form a one-dimensional infinite herring-bone or cuneiform chain structure (Fig. 4a). This herring-bone chain is uncommon as a result of its geometry of structure. Through five kinds of hydrogen bonds (O7–H7B···O1, O7–H7A···O5, O8–H8B···O2, O4–H4···O5, O8–H8A···O3) (Table S1, Supporting Information), the herring-bone chain is further extended to a two-dimensional network (Fig. 4b). Cd2 center is also six-coordinated by two nitrogen atoms from two different 4,4′-bipy ligands (Cd2–N3 2.317 (4) Å, Cd2–N4A 2.324 (3) Å), two oxygen atoms (Cd2–O8 2.368(4) Å, Cd2–O9 2.327 (3) Å) from water molecules, and another two oxygen atoms (Cd2–O10 2.289 (4) Å, Cd2–O11A 2.256 (4) Å) from carboxylate groups. The above carboxylate groups in **2** are the products of decomposition and carbonylation of DMF [39–41]. Two Cd2 ions are bridged by two carboxylate groups with Cd···Cd separations of 4.231 Å to form a dimer unit, which is further interconnected with nitrogen atoms of 4,4′-bipy to form a one-dimensional ladder structure (Fig. 4c). This ladder structure is similar to that found in $[Hg(\mu\text{-}4,4'\text{-bipy})(\mu\text{-AcO})(AcO)]_n$, where metal centers are linked through two acetate anions and 4,4′-bipy [42]. Through the hydrogen bonding (O9–H9A···O6, O9–H9B···O2) (Table S1, Supporting Information) and the above five kinds of hydrogen bonds, the two types of polymeric chains, herring-bone chains and ladder chains, are

Table 2
Selected bond lengths (Å) and angles (deg) for **1–5**.

Complex **1**			
Cd1–O4i	2.292 (3)	N3–Cd1–N1	92.44 (13)
Cd1–N3	2.311 (4)	O2–Cd1–N1	91.16 (12)
Cd1–O2	2.344 (3)	O4i–Cd1–N2ii	86.31 (12)
Cd1–N1	2.358 (3)	N3–Cd1–N2ii	90.58 (13)
Cd1–N2ii	2.365 (3)	O2–Cd1–N2ii	88.83 (12)
Cd1–O1	2.419 (3)	N1–Cd1–N2ii	174.93 (12)
O4–Cd1iii	2.292 (3)	O4i–Cd1–O1	163.08 (11)
N2–Cd1iv	2.365 (3)	N3–Cd1–O1	88.98 (12)
O4i–Cd1–N3	107.94 (12)	O2–Cd1–O1	54.57 (10)
O4i–Cd1–O2	108.54 (11)	N1–Cd1–O1	90.31 (12)
N3–Cd1–O2	143.40 (11)	N2ii–Cd1–O1	93.81 (12)
O4i–Cd1–N1	88.88 (12)		
Complex **2**			
Cd1–N1	2.261 (4)	Cd2–O11ii	2.256 (4)
Cd1–N2	2.289 (5)	Cd2–O10	2.289 (4)
Cd1–O6i	2.320 (3)	Cd2–N3	2.317 (4)
Cd1–O6	2.320 (3)	Cd2–N4iii	2.324 (3)
Cd1–O7i	2.326 (4)	Cd2–O9	2.327 (3)
Cd1–O7	2.326 (4)	Cd2–O8	2.368 (4)
O11–Cd2ii	2.256 (4)	N1–Cd1–N2	180.000 (1)
N1–Cd1–O6i	96.46 (8)	O6i–Cd1–O7i	92.18 (15)
N2–Cd1–O6i	83.54 (8)	O6–Cd1–O7i	87.38 (15)
N1–Cd1–O6	96.46 (8)	N1–Cd1–O7	91.95 (10)
N2–Cd1–O6	83.54 (8)	N2–Cd1–O7	88.05 (10)
O6i–Cd1–O6	167.09 (15)	O6i–Cd1–O7	87.38 (15)
N1–Cd1–O7i	91.95 (10)	O6–Cd1–O7	92.18 (15)
N2–Cd1–O7i	88.05 (10)	O7i–Cd1–O7	176.1 (2)
O11ii–Cd2–O10	117.33 (18)	N3–Cd2–O9	87.35 (13)
O11ii–Cd2–N3	94.66 (15)	N4iii–Cd2–O9	92.57 (13)
O10–Cd2–N3	93.50 (14)	O11ii–Cd2–O8	80.58 (19)
O11ii–Cd2–N4iii	85.67 (15)	O10–Cd2–O8	161.49 (15)
O10–Cd2–N4iii	85.64 (14)	N3–Cd2–O8	89.35 (15)
N3–Cd2–N4iii	179.13 (14)	N4iii–Cd2–O8	91.49 (15)
O11ii–Cd2–O9	162.23 (17)	O9–Cd2–O8	81.79 (15)
O10–Cd2–O9	80.07 (14)		
Complex **3**			
Cd1–N1	2.270 (3)	Cd1–N2i	2.287 (3)
Cd1–O3	2.300 (3)	Cd1–O1	2.317 (3)
Cd1–O4	2.324 (3)	Cd1–O2	2.349 (3)
N2–Cd1ii	2.287 (3)	N1–Cd1–O3	92.83 (10)
N2i–Cd1–O3	87.16 (10)	N1–Cd1–O1	90.22 (10)
N2i–Cd1–O1	90.16 (10)	O3–Cd1–O1	88.67 (10)
N1–Cd1–O4	87.98 (12)	N2i–Cd1–O4	91.64 (11)
O3–Cd1–O4	89.60 (14)	O1–Cd1–O4	177.45 (12)
N1–Cd1–O2	88.97 (10)	N2i–Cd1–O2	91.06 (10)
O3–Cd1–O2	176.15 (9)	O1–Cd1–O2	87.92 (10)
O4–Cd1–O2	93.86 (14)		
Complex **4**			
Cd1–O2	2.298 (5)	Cd1–N1i	2.344 (6)
Cd1–N3	2.332 (6)	Cd1–O1	2.349 (5)
Cd1–N4ii	2.354 (6)	N1–Cd1i	2.344 (6)
Cd1–N2	2.366 (7)	N4–Cd1ii	2.354 (6)
O2–Cd1–N3	89.6 (2)	O2–Cd1–N1i	90.5 (2)
N3–Cd1–N1i	97.0 (2)	O2–Cd1–O1	177.6 (2)
N3–Cd1–O1	91.1 (2)	N1i–Cd1–O1	87.2 (2)
O2–Cd1–N4ii	96.3 (3)	N3–Cd1–N4ii	88.5 (2)
N1i–Cd1–N4ii	171.3 (2)	O1–Cd1–N4ii	85.9 (2)
O2–Cd1–N2	84.0 (2)	N3–Cd1–N2	173.6 (2)
N1i–Cd1–N2	83.0 (2)	O1–Cd1–N2	95.3 (2)
N4ii–Cd1–N2	92.3 (2)		
Complex **5**			
Ag1–N2	2.1597 (18)	Ag1–N1i	2.1642 (19)
Ag1–Ag1ii	3.3449 (4)	N1–Ag1iii	2.1642 (19)
N2–Ag1–N1i	171.02 (8)	N2–Ag1–Ag1ii	78.74 (5)
N1i–Ag1–Ag1ii	109.93 (5)		

Symmetry codes: (1) (i) x, $-1+y$, z; (ii) $1/2+x$, $-y+3/2$, $1/2+z$; (iii) x, $1+y$, z; (iv) $-1/2+x$, $-y+3/2$, $-1/2+z$; (2) (i) $-x$, y, $1/2-z$; (ii) $1/2-x$, $5/2-y$, $1-z$; (iii) $1/2+x$, $-1/2+y$, z; (iv) x, y, z; (v) $-1/2+x$, $1/2+y$, z; (vi) x, $-1+y$, z; (vii) x, $1+y$, z; (3) (i) x, y, $-1+z$; (ii) x, y, $1+z$; (4) (i) $-x$, $2-y$, $-z$; (ii) $-x$, $1-y$, $1-z$; (5) (i) $-1+x$, $-1+y$, z; (ii) $-x$, $1-y$, $-z$; (iii) $1+x$, $1+y$, z.

extended to a three-dimensional structure (Fig. S1, Supporting Information).

4.2.3. $\{[Cd(4,4'\text{-bipy})(H_2O)_4][HL]\cdot H_2O\}_n$ (**3**)

Single-crystal X-ray analysis reveals that one kind of crystallographically unique HL^{2-} anion and one kind of crystallographically unique Cd(II) ion exist in the structure of complex **3**. The HL^{2-} ligand does not coordinate to Cd(II) center, though its $-COOH$ and $-SO_3H$ groups are both deprotonated, and HL^{2-} here only acts as a counter anion for charge balance. Cd1 atom is six-coordinated in a distorted octahedral environment by two nitrogen atoms from different 4,4′-bipy ligands, four oxygen atoms from four water molecules (Fig. 5). The Cd(II) centers are bridged by 4,4′-bipy ligands to form the infinite linear chains and stack themselves to form a two-dimensional network (Fig. S2, Supporting Information). The HL^{2-} anions also stack to a 2D network, as shown in Fig. S3 (Supporting Information). Through complicated hydrogen bonding (Table S2, Supporting Information) among oxygen atoms of carboxylic, sulfonic groups of HL^{2-} and oxygen atoms of coordinated or free water molecules, the polymeric chains and HL^{2-} anion groups stack to form a three-dimensional structure (Fig. 6).

4.2.4. $[Cd(HL)(dpp)_2(H_2O)]_n\cdot 4nH_2O$ (**4**)

A single-crystal X-ray diffraction study reveals that complex **4** adopts a one-dimensional double-stranded chain structure. As depicted in Fig. 7, the asymmetric unit of **4** consists of a single cadmium atom. The Cd1 is six-coordinated by one oxygen atom from sulfonate group of HL^{2-} ligand, one oxygen atom from water molecule, and four nitrogen atoms from unidentate dpp ligands. Cd1 ion displays a distorted octahedral coordination environment. The dpp ligand links Cd(II) centers to yield a double-stranded chain, with the separation of two Cd1 ions being 12.321 Å. Furthermore, π–π interactions appear between the benzene rings of adjacent chains with the center-to-center and face-to-face distances of 3.69 and 3.35 Å, respectively, expanding the double-stranded chains into a 2D network (Fig. 8a). The 2D networks stack along *a*-axis by intermolecular Van der Waals force, as shown in Fig. 8b. Some of coordination complexes with double-stranded chain have been reported, and these chains further form 2D network through π–π interactions, such as Co-sulfosalicylate complex [29].

4.2.5. $\{[Ag(4,4'\text{-bipy})][Hhbs]\}_n$ (**5**)

During the synthetic process of complex **5**, *in situ* decarboxylation of 5-sulfosalicylic acid (H_3L) into 4-hydroxybenzenesulfonic acid (H_2hbs) was involved [43–45], and $Hhbs^-$ anion in **5** acts as a counter-anion for charge balance. There is one crystallographically unique silver ion. Ag1 is coordinated by two nitrogen atoms from different 4,4′-bipy ligands with both Ag1–N2 and Ag1–N1B distances being 2.1596(18) and 2.1642(19) Å, respectively. Moreover, the Ag1–Ag1A distance of 3.3448(4) Å is approximately equal to the Van der Waals contact distance for Ag⋯Ag (3.40 Å). Two chains of alternate Ag1 cations and 4,4′-bipy ligands are connected by the Ag–Ag interactions to form one-dimensional ladder arrays (Fig. 9a), with two chains serving as side rails and Ag–Ag bonds as cross rungs. While the $Hhbs^-$ anions are also linked to a one–dimensional chain by their hydrogen bonding (O4–9A⋯O2: 1.61 (5) Å, O4–O2: 2.695 (3) Å). The chains are further extended to form a two-dimensional network by Van der Waals force (Fig. 9b), and then stack with the above-mentioned ladder arrays in an –ABAB– sequence, as shown in Fig. 10. Although there are a variety of 4,4′-bipy containing metal complexes with ladder motifs, such as $\{[Cu_2(4,4'\text{-bipy})_3(H_2O)_2(4\text{-aba})_2](NO_3)_2(H_2O)_4\}_n$ [46], $[Ag_2(4,4'\text{-bipy})_{1.5}$

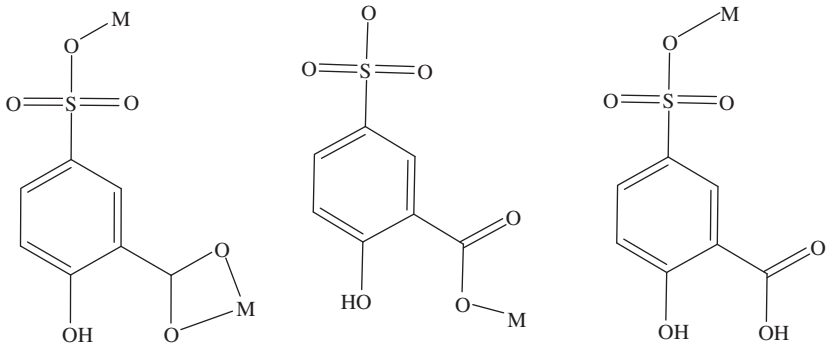

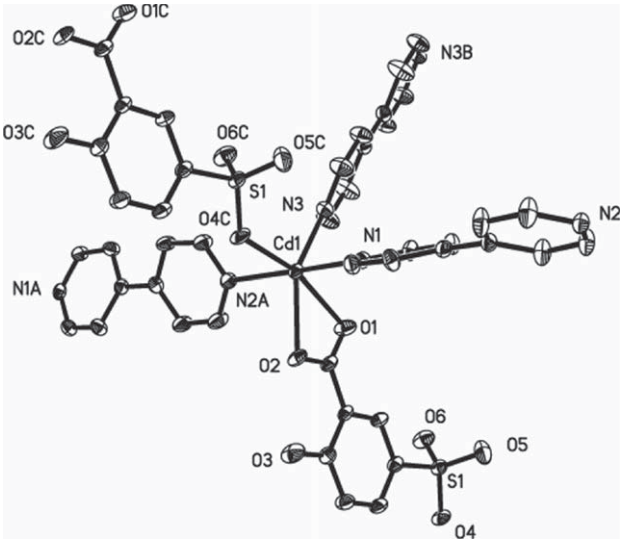

Fig. 1. View of the coordination environments of Cd(II) center of complex **1**. Thermal ellipsoids for the non-hydrogen atoms were drawn at the 30% probability level (A: 1/2+*x*, 3/2−*y*, 1/2+*z*; B: 1/2−*x*, 3/2−*y*.−*z*; C: *x*, *y*−1, *z*).

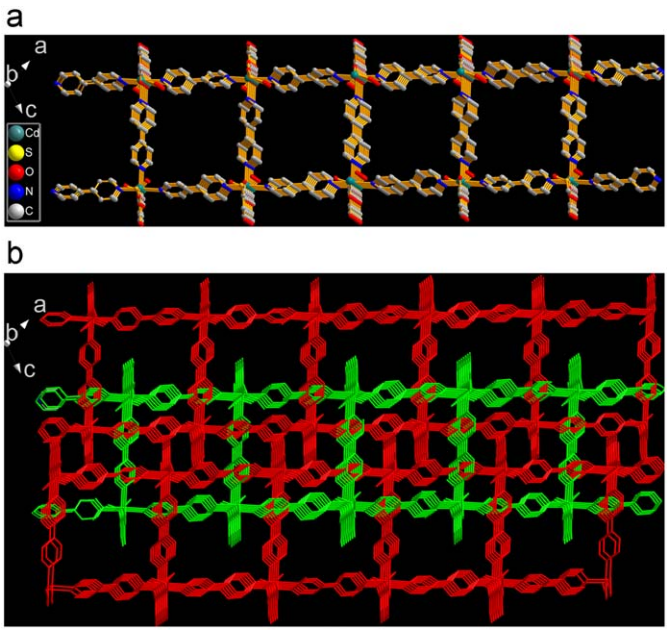

Fig. 2. (a) Two-dimensional network of **1** and (b) three-dimensional supramolecular structure through 2-fold interpenetration along [0, 1, 0] orientation of **1**.

(2-nitroso-1-naphthol-4-sulfonate anion) $(H_2O)]\cdots H_2O$ and $[Ag_2(4,4'\text{-bipy})_2$ (2,6-naphthalenedisulfonate anion) $(H_2O)_2]$ [47], where the organic ligands connect the two adjacent metal ions, few of them have metal–metal bonds or interactions.

4.3. Thermal analyses and PXRD patterns

To investigate their thermal stabilities and decomposition behavior, the thermal gravimetric analyses (TGA) of complexes **1**, **2** and **5** were carried out at the rate of 10 °C/min under nitrogen atmosphere, complexes **3** and **4** carried out at the rate of 10 °C/min under air atmosphere (TGA, Fig. S4, Supporting information). As shown in Fig. 13, complex **1** undergoes a slow mass loss of 3.1% between 30 and 121 °C, with the loss of one molecule H_2O (2.9% calcd). Then the framework is destroyed gradually. Complex **2** seems not as stable as complex **1**. Heating between 133 and 187 °C results in the collapse of complex **2** with a weight loss of 7.5%, implying the loss of six water molecules. For complexes **3** and **4**, the weight loss is 14.01% (calcd 15.66%) and 6.44% (calcd 11.05%) respectively, the deviation may result from loss of partial water molecules from the sample. Complex **3** gives a one-step weight loss between 30 and 132 °C, and then its framework structure starts to collapse, while **4** begins to decompose at 113 °C. Complex **5** collapses under heating at 140 °C. The purity of complexes is confirmed by Powder X-ray diffraction (PXRD, Fig. S5, Supporting

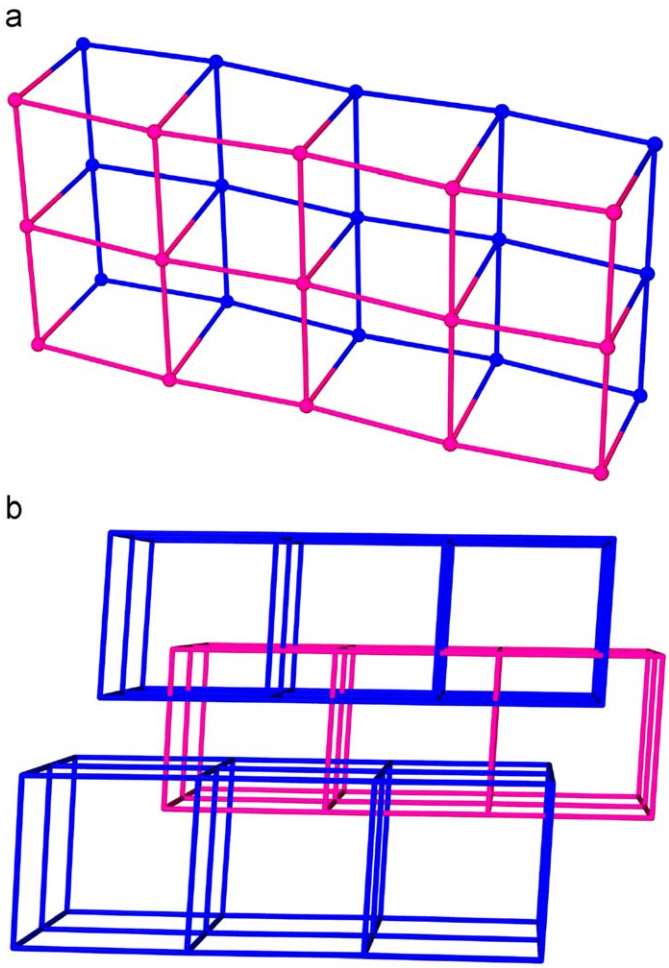

Fig. 3. (a) The 5-connected topological motifs of complex **1**, the 4^4 nets are shown in red and blue and (b) schematic representation of the three-dimensional bilayer network with 2-fold interpenetration. (For interpretation of the references to color in this figure legend, the reader is referred to the webversion of this article.)

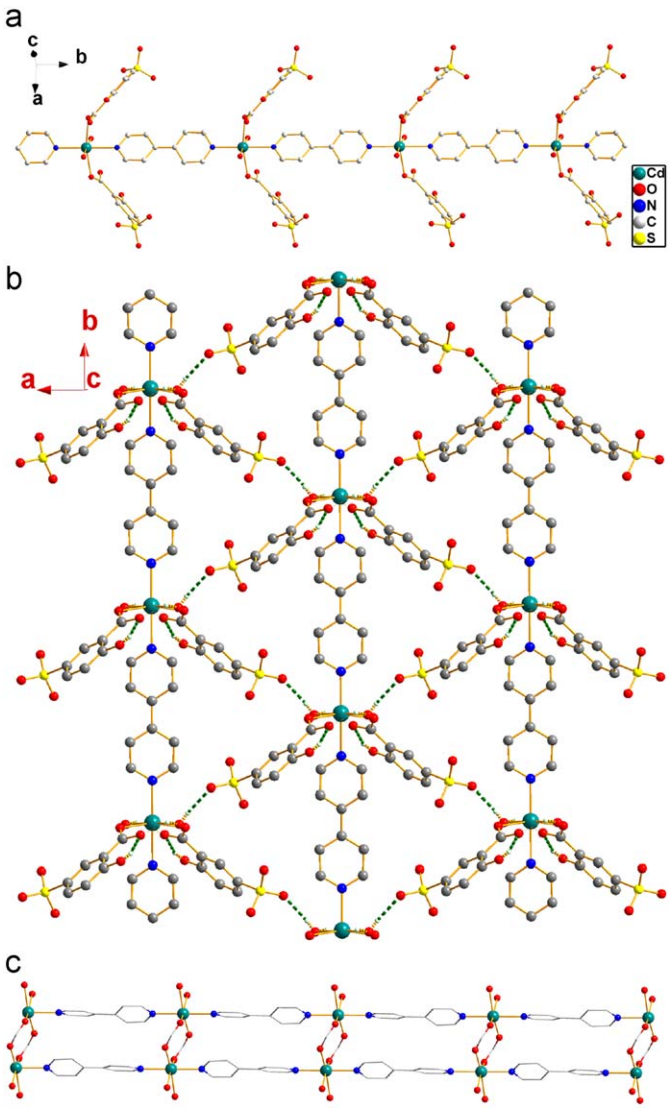

Fig. 4. (a) Herring-bone polymeric chain structure in **2**; (b) view of two-dimensional network from [0,0,1] orientation through hydrogen bonding and (c) ladder structure in **2**.

Information), in which the as-synthesized spectra of complexes **1–4** are almost consistent with their simulated spectra.

4.4. Luminescent properties

Complex **1** exhibits green luminescence at solid state and room temperature, giving broad emission at 542 nm upon excitation at 310 nm, with lifetime (τ) 5.63 ns. The main emission peaks of free H_3L and 4,4′-bipy are at 387 and 425 nm, respectively [29–30,48]. Obviously, the bathochromic shifts of 155 and 117 nm have appeared in complex **1**. The emission spectra are at 554 nm for **3** (λ_{ex}=340 nm, lifetime (τ) 2.84 ns) and at 548 nm for **4** (λ_{ex}=340 nm, lifetime (τ) 1.78 ns), which show high red-shifts compared with their free ligands. While the emission spectrum of **2** also shows a red-shift, but gives the broad band (λ_{max}=509 nm, λ_{ex}=400 nm, lifetime (τ) 4.32 ns) due to the two different Cd(II) centers in **2**. As shown in Fig. 11, all of complexes **1–4** exhibit green luminescences. And, these emissions may be assigned to ligand-to-metal chare transfer (LMCT) from ligand to cadmium [49], since free-ligand emissions for H_3L and ancillary ligands (4,4′-bipy and dpp [50]) are not observable in these four complexes. Complex **5** exhibits blue luminescence with two

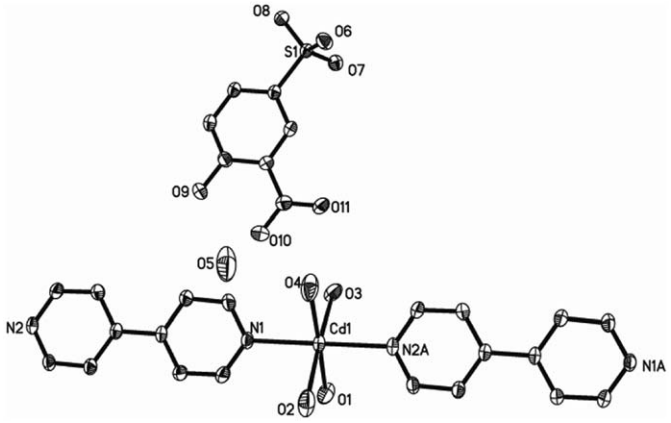

Fig. 5. Molecular species **3**, shown with thermal ellipsoids at 30% probability. All hydrogen atoms have been omitted (A: $x, y, z-1$).

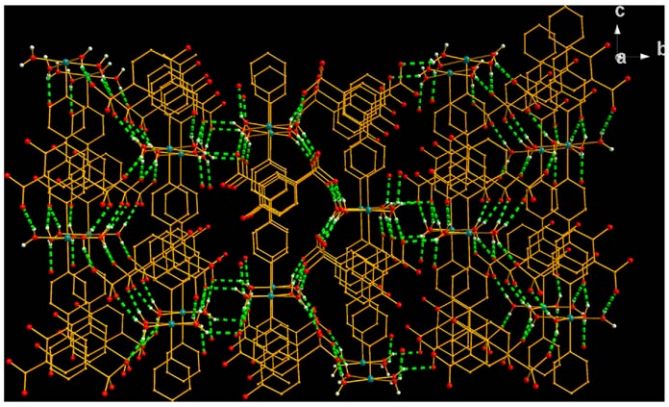

Fig. 6. Perspective views of stacking structure of complex **3** along *a*-axis.

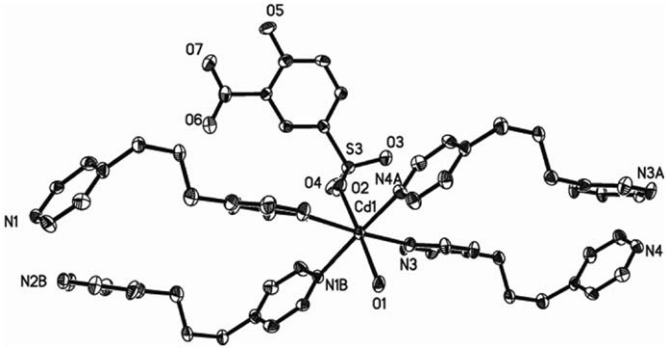

Fig. 7. Perspective view of the coordination environment of the Cd(II) center in **4** (A: $-x, 1-y, 1-z$; B: $-x, 2-y, -z$).

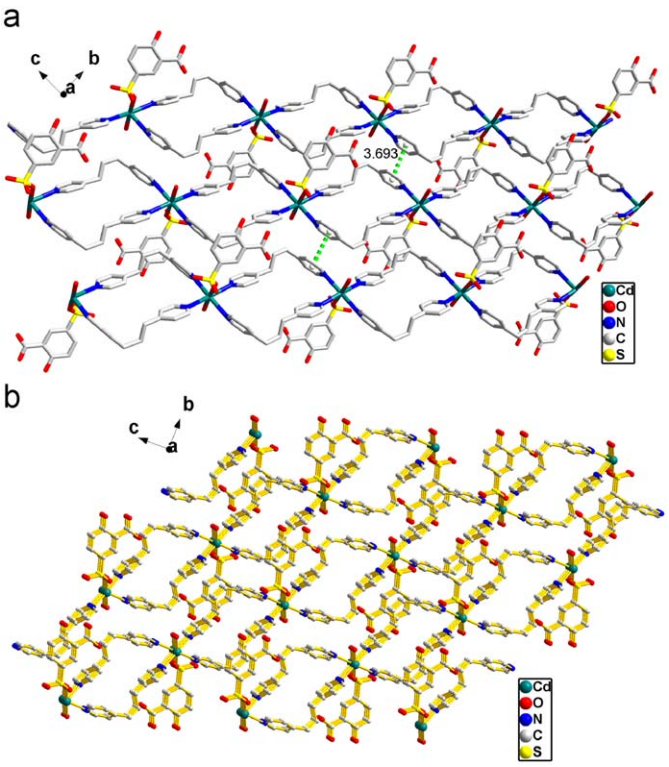

Fig. 8. (a) The $\pi-\pi$ interactions between double-stranded chains along the *b*-axis and (b) stacking structure along *a*-axis in complex **4**.

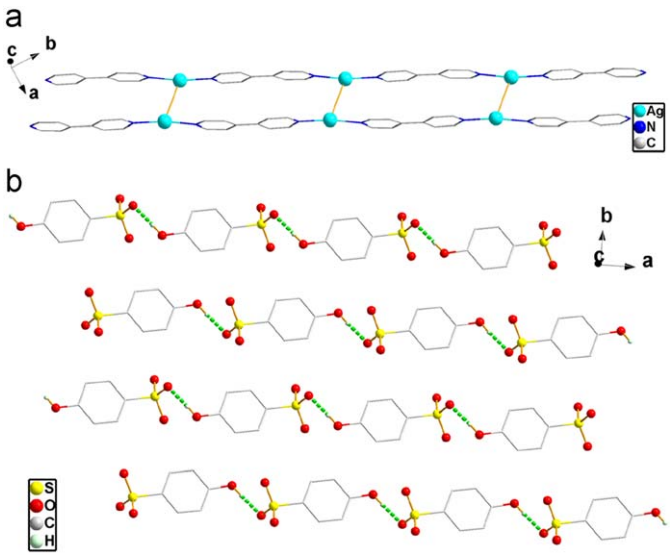

Fig. 9. (a) One-dimensional chain structure of dinuclear silver in **5** and (b) view of two-dimensional network from [0,0,1] orientation through hydrogen bonding and intermolecular Van der Waals force.

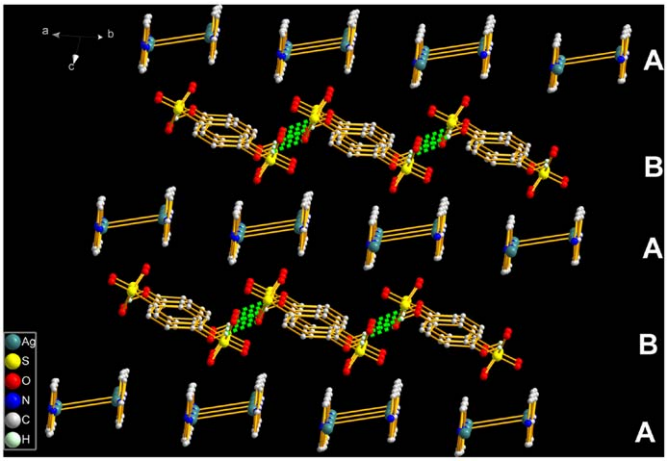

Fig. 10. Stacking modes in –ABAB– sequence for complex **5**.

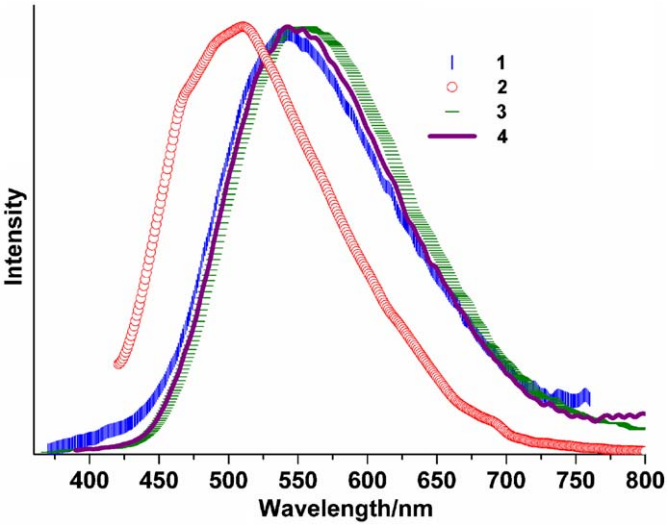

Fig. 11. Solid emission spectra of complexes **1**–**4** at room temperature.

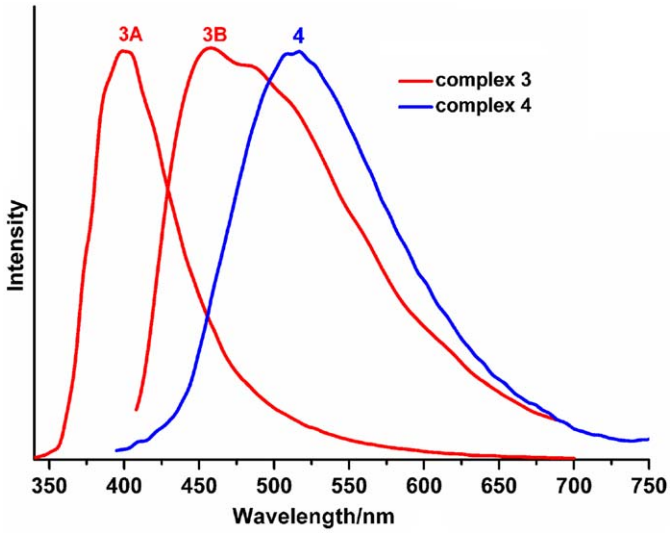

Fig. 12. Solid-state photoluminescent spectra of complex **3** (3A: ex 320 nm; 3B: ex 380 nm) and complex **4** at 10 K.

peaks at 418 and 439 nm upon excitation at 375 nm (Fig. S6, see Supporting Information), with lifetime (τ) 1.04 ns, which are probably due to the π^*–n or π^*–π transition of 4,4′-bipy [48]. For further research, we also study the solid-state photoluminescent spectra of **3** and **4** at 10 K. Interestingly, complex **3** exhibits two kinds of emission spectra when excited by two different excitation wavelengths. Complex **3** shows violet luminescence, giving intense emission at 399 nm upon excitation at 320 nm, with lifetime (τ) 6.15 ns, while it also exhibits cyan luminescence, giving broad emissions at 457 and 490 nm upon excitation at 380 nm, with lifetime (τ) 8.74 ns. The former emission (399 nm) may originate from $\pi \rightarrow \pi^*$ transition of the ligand (H_3L, 387 nm) [30,32], and the later broad emissions (457, 490 nm) can be attributed to the $^1\pi$, π^* state of the 4,4′-bipy ligand [51]. The above two kinds of emission spectra both show obvious blue-shifts compared with emission spectrum of **3** at room temperature (Fig. 12). Complex **4** shows green luminescence, giving broad emission at 515 nm (λ_{ex}=346 nm, lifetime (τ) 16.7 ns). It also shows lower blue-shifts compared with its emission spectrum at room temperature (Fig. 12).

5. Conclusions

In summary, reactions of 5-sulfosalicylic acid and d^{10} transition metal ions (Cd^{II}, Ag^{I}) in the presence of N-donor ligands produce a series of d^{10} metal-sulfosalicylate coordination polymers with the interesting structures. For all the complexes, the N-donor ligands, hydrogen-bonding interactions, π–π interactions and intermolecular Van der Waals force play the important roles in the formation of supramolecular architectures. Complexes **1–3** form three-dimensional supermolecular structures, in which **1** adopts 5-connected bilayer topology, and **2** has aesthetic herring-bone and ladder-like chain framework. While complexes **4–5** possess two-dimensional structures, where **4** is built from double-stranded chains, and **5** consists of ladder arrays.

In addition, complexes **1–4** exhibit green luminescences in solid state at room temperature, while emission spectra of **3** and **4** show obvious blue-shifts at low temperature, all of which could be significant in the field of luminescent materials.

Supplementary material

Crystallographic data for the five complexes in this paper have been deposited at the Cambridge Crystallographic data center, CCDC nos. 715305, 715306, 715307, 715308 and 715309 are for complexes **1–5**, respectively. These data can be obtained free of charge at http://www.ccdc.cam.ac.uk/conts/retrieving-.html (or from the Cambridge Crystallographic Data Center, 12 Union Road, Cambridge CB2 1EZ, UK; fax: +44 1223 336 033; e-mail: deposit@ccdc.cam.ac.uk).

Acknowledgments

This work was supported by 973 Program (2006CB932900), the National Natural Science Foundation of China, and Natural Science Foundation of Fujian Province (2007J172).

Appendix A. Supplementary material

Supplementary data associated with this article can be found in the online version at 10.1016/j.jssc.2009.08.025.

References

[1] B. Moulton, M.J. Zaworotko, M.J. Zaworotko, Chem. Rev. 101 (2001) 1629.
[2] O.R. Evans, R. Xiong, Z. Wang, G.K. Wong, W. Lin, Angew. Chem. Int. Ed. 38 (1999) 557.
[3] M. Eddaoudi, D.B. Moler, H.L. Li, B.L. Chen, T.M. Reineke, M. O'Keeffe, O.M. Yaghi, Acc. Chem. Res. 34 (2001) 319.
[4] O.R. Evans, R.G. Xiong, Z.Y. Wang, G.K. Wong, W.B. Lin, Angew. Chem. Int. Ed. 38 (1999) 536.
[5] F.Y. Lian, F.L. Jiang, D.Q. Yuan, J.T. Chen, M.Y. Wu, M.C. Hong, CrystEngComm 10 (2008) 905.
[6] S.S. Sun, A.J. Lees, Coord. Chem. Rev. 230 (2002) 170.
[7] C. Janiak, Dalton Trans. (2003) 2781.
[8] B. Zhao, X.Y. Chen, P. Cheng, D.Z. Liao, S.P. Yan, Z.H. Jiang, J. Am. Chem. Soc. 126 (2004) 15394.
[9] L. Han, Y.Q. Gong, D.Q. Yuan, M.C. Hong, J. Mol. Struct. 789 (2006) 128.
[10] G.M. Cockrell, G. Zhang, D.G. VanDerveer, R.P. Thummel, R.D. Hancock, J. Am. Chem. Soc. 130 (2008) 1420.
[11] E.M. Boon, J.K. Barton, Curr. Opin. Struct. Biol. 12 (2002) 320.
[12] C.R. Treadway, M.G. Hill, J.K. Barton, Chem. Phys. 281 (2002) 409.
[13] K. Ishida, T.B. Asao, Biophys. Acta 1587 (2002) 155.
[14] N. Taieb, N. Yahi, J. Fantini, Adv. Drug Deliv. Rev. 56 (2004) 779.
[15] L.L. Miller, K.R. Mann, Acc. Chem. Res. 29 (1996) 417.
[16] P. Leclere, E. Hennebicq, A. Calderone, P. Brocorens, A.C. Grimsdale, K. Mullen, J.L. Bredasm, R. Lazzaroni, Prog. Polym. Sci. 28 (2002) 55.
[17] C. Schmuck, W. Wienand, Angew. Chem. Int. Ed. 40 (2001) 4363.
[18] W. Wei, M.Y. Wu, Y.G. Huang, Q. Gao, Q.F. Zhang, F.L. Jiang, M.C. Hong, CrystEngComm 11 (2009) 576.
[19] O. Ermer, Adv. Mater. 3 (1991) 608.
[20] M.L. Głowka, D. Martynowski, K. Kozłowska, J. Mol. Struct. 474 (1999) 81.
[21] L. Pan, N.W. Zheng, N.W. Wu, X.Y. Huang, J. Coord. Chem. 47 (1999) 551.
[22] C.A. Hunter, Chem. Soc. Rev. 23 (1994) 101.
[23] T. Steiner, Angew. Chem. Int. Ed. 41 (2002) 48.
[24] C.S. Liu, X.S. Shi, J.R. Li, J.J. Wang, X.H. Bu, Cryst. Growth Des. 6 (2006) 656.
[25] G.M. Whitesides, J.P. Mathias, C.T. Seto, Science 254 (1991) 1312.
[26] G.R. Desiraju, Acc. Chem. Res. 35 (2002) 565.
[27] Y.H. Wan, L.P. Zhang, L.P. Jin, S. Gao, S.Z. Lu, Inorg. Chem. 42 (2003) 4985.
[28] D. Bose, J. Banerjee, Sk.H. Rahaman, G. Mostafa, H.K. Fun, R.D.B. Walsh, M.J. Zaworotko, B.K. Ghosh, Polyhedron 23 (2004) 2045.
[29] Z.D. Lu, L.L. Wen, Z.P. Ni, Y.Z. Li, H.Z. Zhu, Q.J. Meng, Cryst. Growth Des. 7 (2007) 268.
[30] F.F. Li, J.F. Ma, S.Y. Song, J. Yang, Cryst. Growth Des. 6 (2006) 209.
[31] S.R. Fan, L.G. Zhu, Inorg. Chem. 46 (2007) 6785.
[32] S.R. Fan, L.G. Zhu, Inorg. Chem. 45 (2007) 7935.
[33] Z.D. Lu, L.L. Wen, J. Yao, H.Z. Zhu, Q.J. Meng, CrystEngComm 8 (2006) 847.
[34] J.F. Ma, J. Yang, S.L. Li, S.Y. Song, Cryst. Growth Des. 5 (2005) 807.
[35] P.S. Rao, D.N. Sathyanarayana, S. Palaniappan, Macromolecules 35 (2002) 4988.
[36] G.M. Sheldrick, SHELXS97, Program for Crystal Structure Solution, University of Gottingen, Gottigen, Germany, 1997.
[37] G.M. Sheldrick, SHELXL97, Program for Crystal Structure Refinement, University of Gottingen, Gottigen, Germany, 1997.

[38] J.F. Song, Y. Chen, Z.G. Li, R.S. Zhou, X.Y. Xu, J.Q. Xu, T.G. Wang, Polyhedron 26 (2007) 4397.
[39] A.C. Sudik, A.P. Côté, A.G. Wong-Foy, M. O'Keeffe, O.M. Yaghi, Angew. Chem. Int. Ed. 45 (2006) 2528.
[40] Y.S. Varshavsky, T.G. Cherkasova, J. Org. Chem. 692 (2007) 887.
[41] P. Serp, M. Hernandez, B. Richard, P. Kalck, Eur. J. Inorg. Chem. (2001) 2327.
[42] G. Mahmou, A. Morsali, A.D. Hunter, M. Zeller, Inorg. Chim. Acta 360 (2007) 3196.
[43] Y.Z. Zheng, Y. B Zhang, M. L Tong, W. Xue, X.M. Chen, Dalton Trans. (2009) 1396.
[44] X.M. Zhang, Coord. Chem. Rev. 249 (2005) 1201.
[45] X.M. Zhang, R.Q. Fang, Inorg. Chem. 44 (2005) 3955.
[46] R.H. Wang, F.L. Jiang, Y.F. Zhou, L. Han, M.H. Hong, Inorg. Chim. Acta 358 (2005) 545.
[47] H. Wu, X. Wu Dong, H.Y. Liu, J.F. Ma, S.L. Li, J. Yang, Y.Y. Liu, Z.M. Su, Dalton Trans. (2008) 5331.
[48] G. Tian, G.S. Zhu, Q.R. Fang, X.D. Guo, M. Xue, J.Y. Sun, S.L. Qiu, J. Mol. Struct. 787 (2006) 45.
[49] W.G. Lu, L. Jiang, X.L. Feng, T.B. Lu, Cryst. Growth Des. 6 (2006) 564.
[50] Q.Y. Liu, L. Xu, CrystEngComm 7 (2005) 87.
[51] X.M. Zhang, M.L. Tong, M.L. Gong, X.M. Chen, Eur. J. Inorg. Chem. (2003) 138.